Experimental Investigation of a Finned-tube Heat Exchangers with a Phase Change Material for Thermal Energy Storage

Łukasz Lis[a], Wojciech Kalawa[a], Ewelina Radomska[a] Andrzej Gołdasz[a], Marta Kuta[a], Łukasz Mika[a], Agata Mlonka-Mędrala[a], Artur Szajding[b] and Karol Sztekler[a]

[a] AGH University of Krakow, Faculty of Energy and Fuels, Department of Thermal and Fluid Flow Machines, Krakow, Poland, radomska@agh.edu.pl (CA), kalawa@agh.edu.pl, llis@agh.edu.pl, goldasz@agh.edu.pl, marta.kuta@agh.edu.pl, lmika@agh.edu.pl, amlonka@agh.edu.pl, sztekler@agh.edu.pl

[b] AGH University of Krakow, Faculty of Metals Engineering and Industrial Computer Science, Department of Heat Engineering and Environment Protection, Krakow, Poland, artur.szajding@agh.edu.pl

Abstract:

Thermal energy storage (TES) systems play a critical role in enhancing the flexibility, stability and overall efficiency of modern energy systems, particularly those integrating high shares of intermittent renewable energy sources. Among TES methods, latent heat storage using phase change materials (PCMs) is especially attractive due to its ability to store large amounts of energy within a narrow temperature range, thereby reducing system size, limiting heat losses, and improving operational predictability. Solid–liquid PCMs are of particular interest because they combine high latent heat with negligible (as compared to solid-gas or liquid gas PCMs) volumetric changes during melting and solidification. Nevertheless, the inherently low thermal conductivity of most PCMs significantly limits heat transfer rates, leading to extended charging and discharging times and constraining the achievable power density of TES units. To overcome this limitation, various heat exchanger enhancements have been proposed, with fin-based structures being among the most effective solutions.

This study presents a comprehensive experimental investigation of four finned-tube heat exchanger configurations designed to improve heat transfer performance in a PCM-based TES system. The system employed a commercially available PCM (A82, Phase Change Material Products Limited, UK), with approximately 10 kg of material stored in a stainless-steel tank containing an internal copper heat transfer fluid (HTF) tube. The tested configurations included: (a) seven straight alumina fins, (b) fourteen straight alumina fins, (c) seven C-shaped alumina fins, and (d) twenty-one straight alumina fins combined with lowered HTF tubes to enhance heat transfer during both melting and solidification. Particular attention was given to the influence of fin number, geometry, and positioning on the spatial distribution of temperature fields within the PCM, as well as the power of the TES system during charging and discharging.

The results demonstrate that increasing the number of fins significantly enhances heat transfer within the PCM, reducing melting and solidification times and increasing the power output of the heat exchanger. These findings contribute to a deeper understanding of how fin geometry and arrangement influence heat transfer mechanisms in PCM-based storage, offering valuable insights for the engineering of more compact and responsive TES units. Moreover, the experimental data generated in this work support the development of more accurate numerical models, which are essential for designing efficient large-scale thermal energy storage systems in future low-carbon energy networks.

Keywords:

Fin; Heat exchanger; Heat transfer; Phase change material; Thermal energy storage

1. Introduction

Thermal energy storage (TES) systems are essential for improving the flexibility, reliability, and efficiency of contemporary energy systems, particularly those with a high share of variable renewable energy sources [1]. Among the available TES technologies, latent heat storage based on phase change materials (PCMs) is especially promising, as it enables the storage of significant amounts of energy within a relatively narrow temperature interval. This allows for more compact system designs, reduced thermal losses, and more predictable operation.

Solid–liquid PCMs are of particular interest due to their high latent heat capacity and relatively (as compared to liquid-gas or solid-gas PCMs) small volume changes during phase transitions. However, a major drawback of most PCMs is their low thermal conductivity, which limits heat transfer rates [2]. As a result, charging and discharging processes are prolonged, and the achievable power output of TES systems is restricted. To address this issue, various design improvements to heat exchangers have been proposed.

Research on heat exchangers for applications involving PCMs is extensive. A search in Google Scholar using the keywords “PCM” and “heat exchanger” yields approximately 8,900 results, highlighting the significant scientific interest in this field. To date, a wide variety of heat exchanger configurations have been proposed in the literature, ranging from simple double-tube [3] and triple-tube [4] designs, through shell-and-tube systems [5], to plate heat exchangers [6]. Moreover, numerous heat transfer enhancement techniques have been investigated, including modifications to the geometry and dimensions of the heat exchanger [7], as well as changes in its orientation angle [8]. Nevertheless, one of the simplest and most effective methods for enhancing heat transfer is to increase the heat transfer surface area by incorporating fins [9].

Rashid et al. [10] reported that the charging time of a TES unit equipped with a heat exchanger without fins was 290 minutes. However, when 4 and 8 fins were applied, the charging time decreased to 120 minutes and 54 minutes, respectively. Similar conclusions can be drawn for the PCM solidification process. For instance, Pássaro et al. [11] found that the solidification time was 188 minutes, 77 minutes, and 45 minutes when the number of fins was 25, 50, and 100, respectively.

Another approach to enhancing heat transfer in PCM systems involves lowering the tubes through which the heat transfer fluid flows. For example, Mase et al. [3] demonstrated that lowering the tube can reduce the charging time of the TES unit by up to 71.7%. However, this modification negatively affects the discharging process (PCM solidification), increasing its duration by 57.8% compared to the concentric tube configuration.

In light of the above, the present study focuses on the experimental investigation of the performance of four different heat exchangers integrated with a PCM-based TES system. The analyzed units are finned-tube heat exchangers, differing in the number of fins, fin geometry, and the position of the tubes carrying the heat transfer fluid.

2. Methodology

The diagram of the test bench is shown in **Figure 1**, while its photograph is presented in **Figure 2**. The primary component under investigation is a TES unit, consisting of a replaceable heat exchanger embedded in a PCM and enclosed within an insulated casing. The remaining components form part of a system designed to maintain stable measurement conditions; these include hot and cold water buffer tanks, pumps, solenoid valves, heaters, coolers, and electronically controlled three-way valves. Also, the test bench included the appropriate measuring devices (**Table 1**). During the experiment, the inlet and outlet temperatures of the working fluid, as well as the flow rate, were monitored. These parameters were regulated using appropriately tuned proportional–integral–derivative (PID) control values.

The system operated in two modes: charging and discharging. In both modes, the working fluid (water) flowed at a rate of 4.7 L/min, corresponding to an average design velocity of 1.0 m/s. During the charging process, the working fluid inlet temperature was 97 ± 1 °C. During discharging, this parameter was reduced to 50 ± 1 °C.

In accordance with the design specifications, A82 (PCM Products Ltd., Great Britain) was selected as the reference PCM. This material has a phase change temperature of 82 °C and a specific latent heat of 240 kJ/kg [12]. The mass of the material involved in the thermal energy storage process was 10 kg.

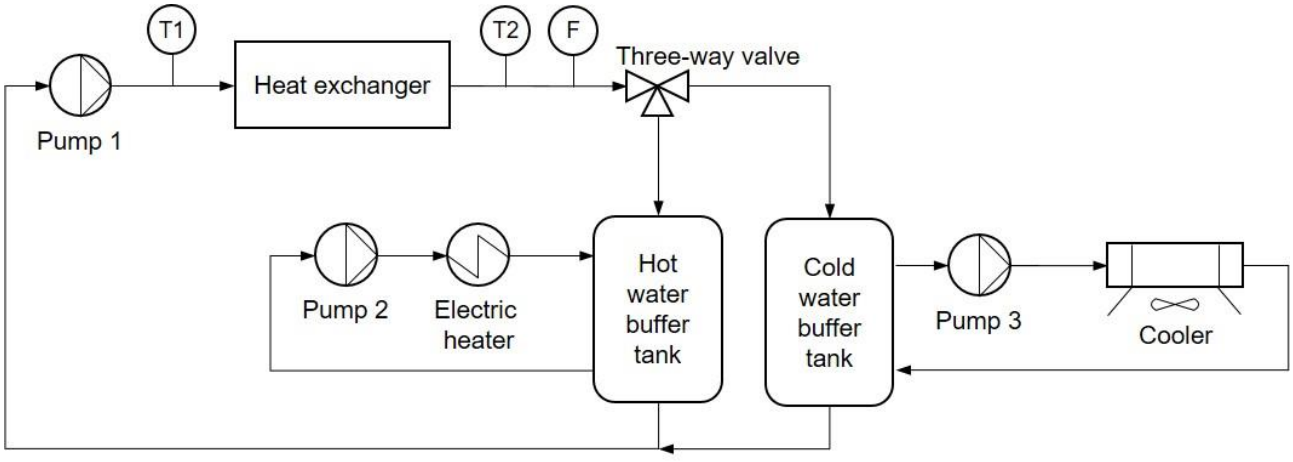

Figure 1. *The diagram of the test bench. T – temperature sensor; F – flow rate sensor.*

Figure 2. *A photograph of the test bench.*

In the described TES unit containing the PCM, temperature sensors were installed to measure the temperature distribution inside the heat exchanger, as shown in **Figure 3**. During the experimental campaign, in the charging cycles, the system was heated until the lowest temperature recorded by the sensors inside the storage unit reached 92 °C. According to preliminary observations, this condition corresponds to a state in which the entire PCM within the storage unit has fully melted. During the discharging cycles, the storage unit was cooled by extracting heat until the highest measured temperature dropped to 70 °C. This condition corresponds to a state in which the entire material inside the heat exchanger has solidified.

Each measurement was repeated three times to verify repeatability. Between measurement series, additional conditioning runs were conducted to ensure consistent initial conditions for all tested configurations. To verify the accuracy of the measurement equipment, each tested heat exchanger was also examined in a configuration where water (approximately 13 kg) was used instead of the PCM.

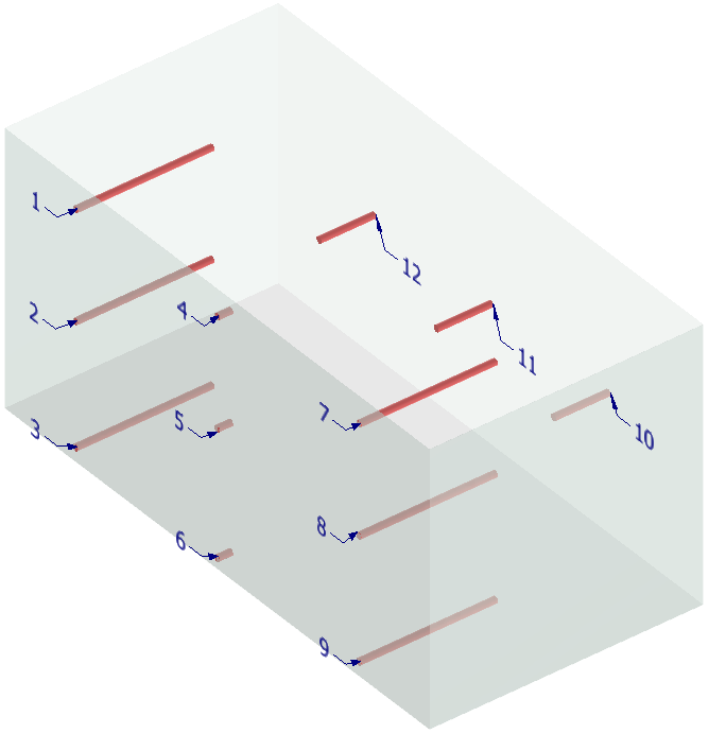

Figure 3. *Location and labelling of temperature sensors inside the thermal energy storage unit (schematic diagram – scale and dimensions not shown).*

In the experiment, four heat exchanger designs were investigated, differing in the number, geometry, and arrangement of fins. The spacing of the fins and the tubes through which the heat transfer fluid flowed is

illustrated in **Figure 4** (heat exchanger A), **Figure 5** (heat exchanger B), **Figure 6** (heat exchanger C), **Figure 7** (heat exchanger D). For the most promising design, heat losses were determined and incorporated into a model describing the relationship between thermal power and the state of charge of the storage unit.

The study constitutes part of a broader research project and aimed to obtain temperature and power characteristics during both charging and discharging processes. These results will serve as a basis for subsequent numerical analyses focused on optimizing the heat exchanger design.

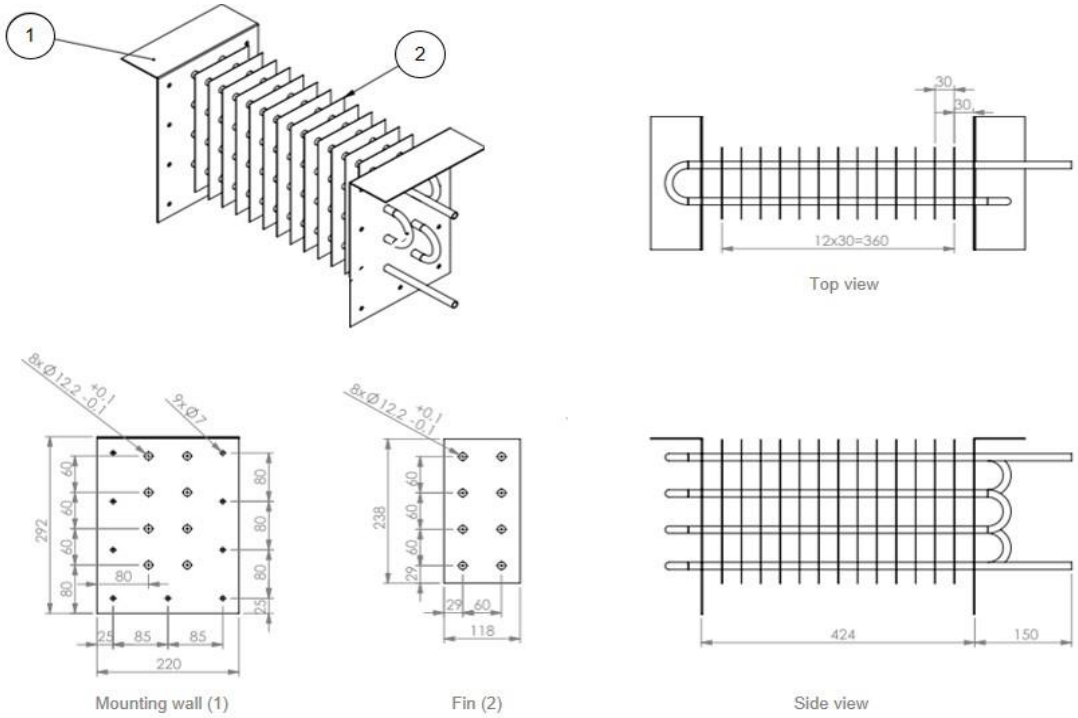

Figure 4. *The first heat exchanger – heat exchanger A.*

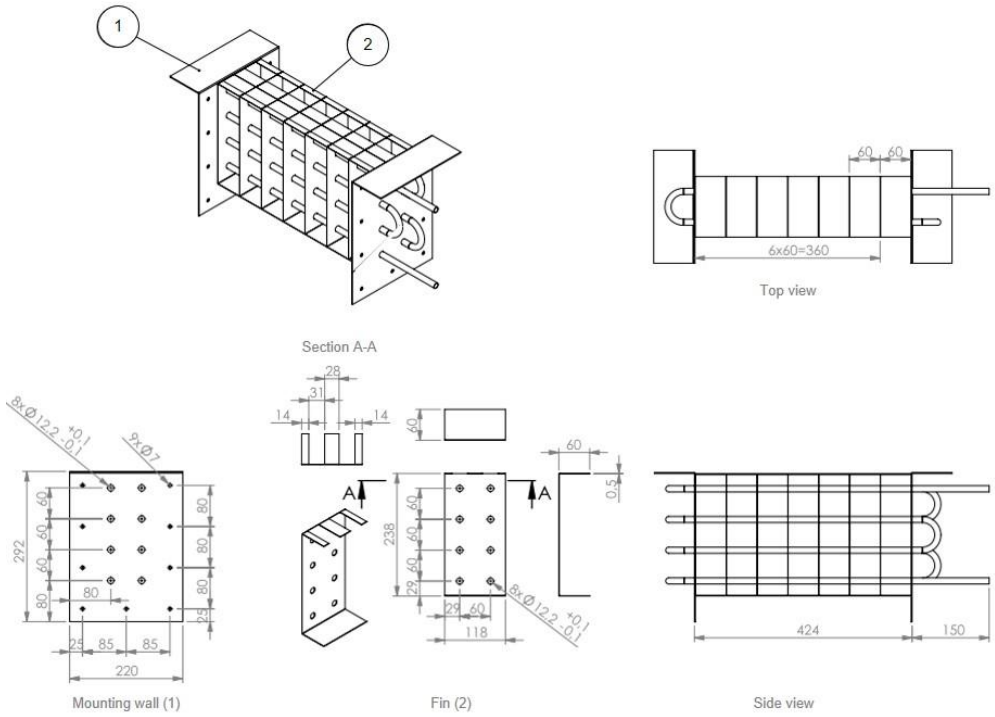

Figure 5. *The second heat exchanger – heat exchanger B.*

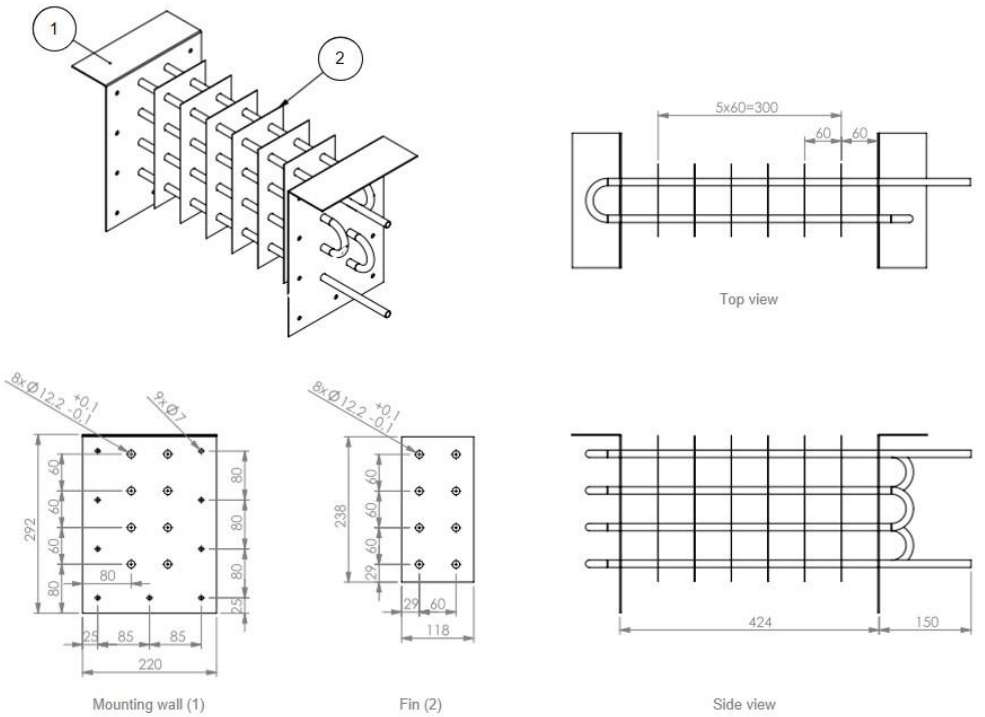

Figure 6. *The third heat exchanger – heat exchanger C.*

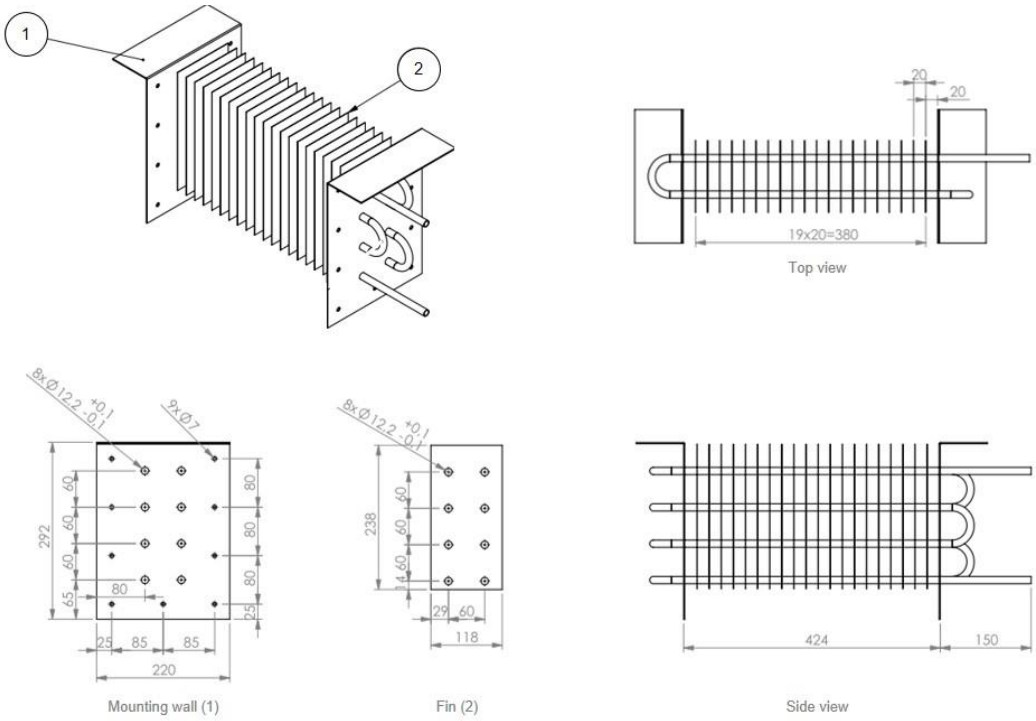

Figure 7. *The fourth heat exchanger – heat exchanger D.*

Table 1. *Measuring devices.*

Measured value	Device	Measuring range	Uncertainty
Temperature	Resistance temperature detector Pt100 TOP-PDm-98 (ALF-SENSOR sp. j., Zabierzów, Poland)	0 – 150 °C	±(0,3+0,005·|t|)
Flow rate	Flow meter JUMO flowTrans MAG I02 (JUMO GmbH&Co. KG, Fulda, Germany)	0,2 – 10 m/s	±3,5% of measured value

3. Results and discussion

3.1. Charging process

Among the tested heat exchangers, only heat exchanger C did not complete the charging process, as the minimum temperature of the PCM in this case did not reach the required 92 °C within 15 hours (see **Figure 8**). The most probable reason for this result is the insufficient heat transfer surface area. Therefore, heat exchanger C will not be considered in the further analysis of the results.

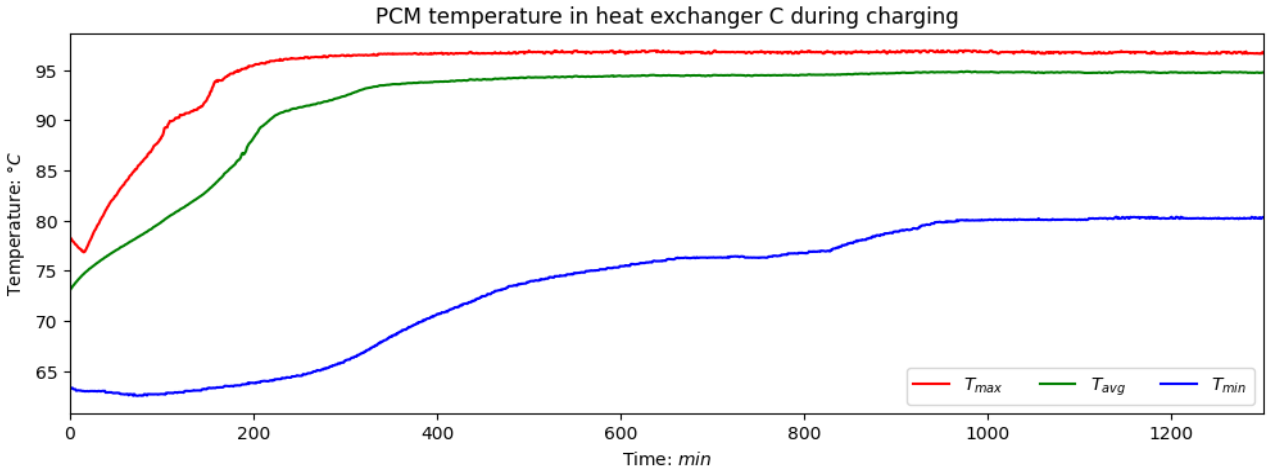

Figure 8. *The maximum (T_{max}), average (T_{avg}) and minimum (T_{min}) PCM temperature in heat exchanger C during charging.*

The time dependence of the maximum (T_{max}), average (T_{avg}), and minimum (T_{min}) PCM temperatures measured in heat exchangers A, B, and D during the charging process is presented in **Figure 9**. During the charging cycles, all of the aforementioned temperatures increased; however, this increase was not uniform. Neither T_{max} nor T_{min} was consistently recorded by a single sensor; instead, their locations varied over the course of the experiment. In all heat exchangers, the fastest temperature increase was observed in the upper section of the heat exchanger, specifically at the sensor located along axis (location 7 in **Figure 3**), while the slowest increase occurred at the sensor positioned near the wall at the bottom (location 6 in **Figure 3**). This behavior is most likely associated with the significant influence of convection on heat transfer, as the heated fluid naturally rises toward the top.

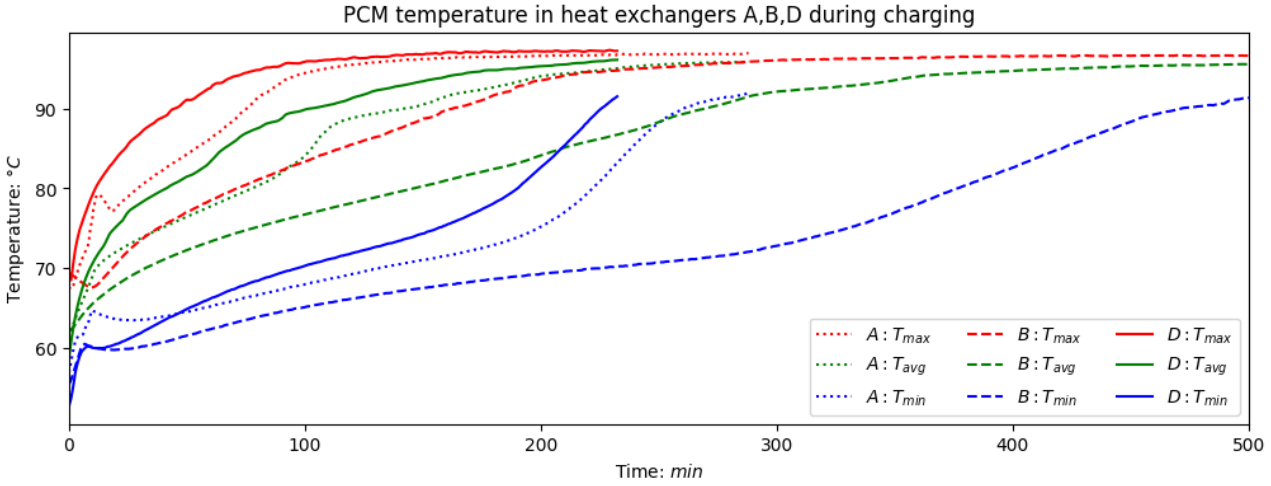

Figure 9. *The maximum (T_{max}), average (T_{avg}) and minimum (T_{min}) PCM temperature in heat exchangers A, B, and D during charging.*

During the experiments, a sudden temperature spike was observed, deviating from the general trend, followed by a drop to the expected values approximately 10 minutes after the start of the test. Initially, this was suspected to be a sensor error within a specific temperature range; however, this hypothesis was not confirmed during control experiments conducted with the storage unit filled with water (**Figure 10**), which did not show any anomalies. However, the abovementioned anomaly obtained in the tests with PCM was reproducible in repeated trials. Further observation revealed a correlation between the onset of PCM melting and the return of temperature readings to expected values. It was ultimately concluded that the abrupt temperature increase was caused by air voids (**Figure 11**), which – due to their lower heat capacity – heated up more rapidly than

the PCM and were subsequently filled with a colder PCM during the heating process. These voids formed during the cooling cycle as a result of significant volumetric contraction (approximately 20%) during solidification of the PCM.

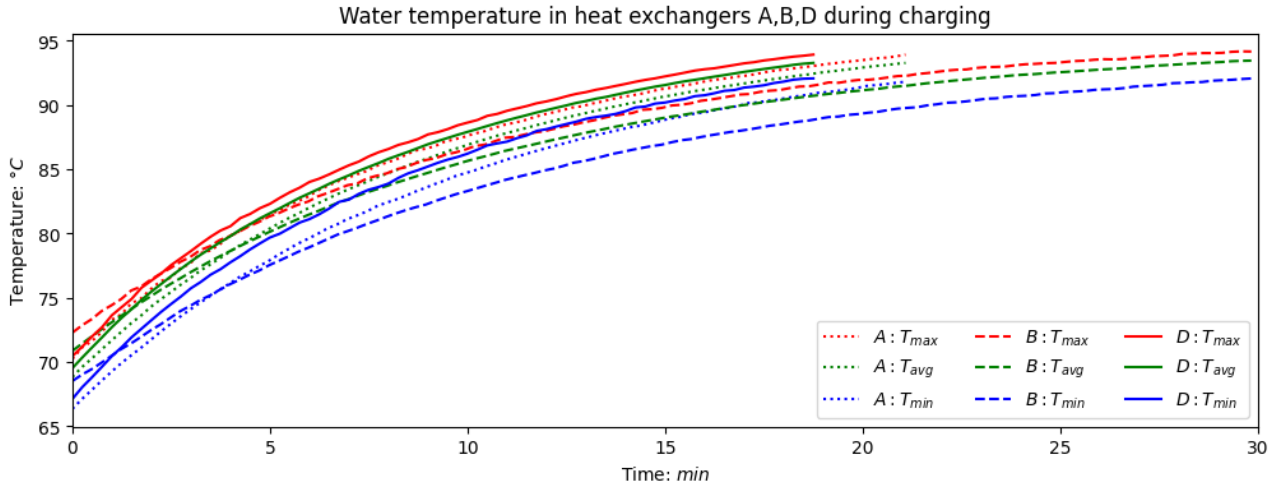

Figure 10. *The maximum (T_{max}), average (T_{avg}) and minimum (T_{min}) water temperature in heat exchangers A, B, and D during a control test.*

Figure 11. *Air voids in the PCM.*

Comparing the designs of heat exchangers, it was found that the variation in the number of fins affected the temperature profiles. As the number of fins increased (heat exchanger D), the maximum temperatures rose significantly faster. Also, T_{max} rose faster than T_{min} and stabilized at approximately 95–96 °C. At the same time, the characteristic plateau in the temperature curve typically associated with phase change in PCM was not observed for T_{max} whereas it was clearly visible for T_{min}. As mentioned earlier, this is likely related to convective effects. The number of fins affected also the charging time which was 288 min, 506 min, and 232 min in the case of heat exchangers A, B, and D, respectively.

Based on the changes in inlet and outlet temperatures and the flow rate of the working fluid, the heat flux transferred to the heat exchanger was calculated using the formula $\dot{Q} = \dot{V} \cdot c_p \cdot \rho \cdot (T_{out} - T_{in})$. where $\dot{V}$ is the measured volumetric flow rate (m^3/s), c_p is the specific heat capacity of water (kJ/(kgK)), ρ is the density of water (kg/m^3), while T_{out} and T_{in} denote the measured outlet and inlet temperatures of the working fluid (°C), respectively. The specific heat capacity and density of the water were taken from [13].

The heat flux, presented in **Figure 12**, is highest at the initial stage of the process, reaching values from approximately 1.7 kW for heat exchanger B, to 3.0 kW for heat exchanger D. As the process continues, the heat flux decreases in an asymptotic manner – marked by a rapid initial drop followed by a gradual stabilization toward a value close to 0 kW. After the initial state of charging (first 50 min), no substantial differences were identified between the analyzed heat exchanger configurations, since the heat flux transferred from the working fluid to the PCM is used to balance the heat losses from the TES unit. The heat losses are comparable in all investigated heat exchangers.

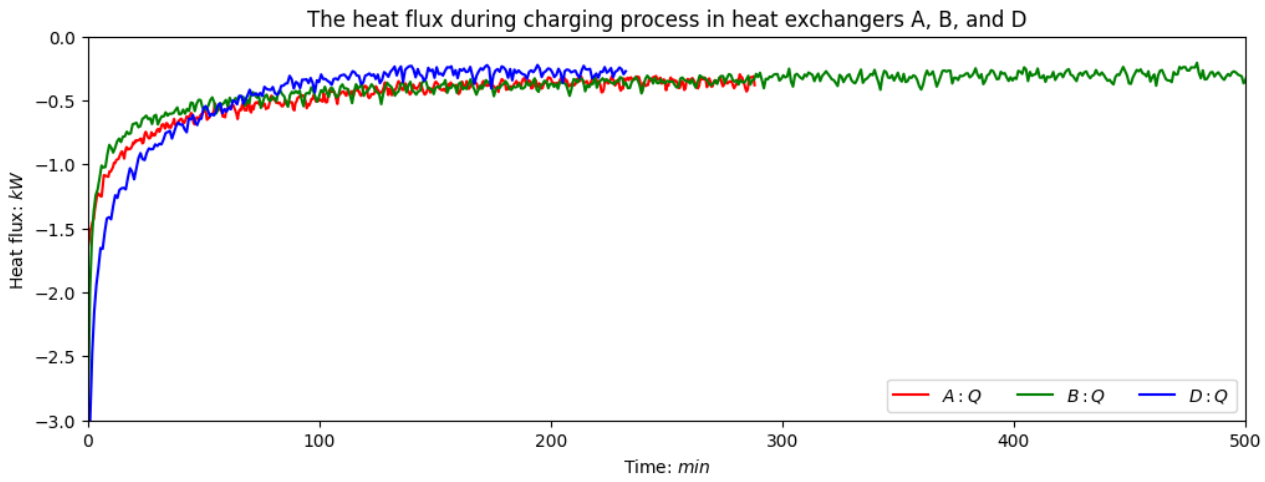

Figure 12. *The heat flux during charging process in heat exchangers A, B, and D.*

3.2. Discharging process

The time dependence of the maximum (T_{max}), average (T_{avg}), and minimum (T_{min}) PCM temperatures measured in heat exchangers A, B, and D during the discharging process is presented in **Figure 13**

The discharging process was shorter than the charging process. The differences were observed both in relative terms (from 2.9 for heat exchanger D to 3.6 for heat exchanger B) and in absolute terms. Moreover, the discrepancy between charging and discharging times increased as the number of fins decreased. This behavior can most likely be attributed to the fact that heat losses from the TES unit support the discharging process, while acting in the opposite direction during charging. Similarly, convective effects promote additional mixing within the PCM, thereby accelerating the process. The characteristic inflection associated with PCMs is visible in all temperature profiles, although with varying intensity. During discharging, the PCM adhered to the cold surfaces, leading to the formation of the previously mentioned air voids. The size of these voids increased with increasing fin spacing.

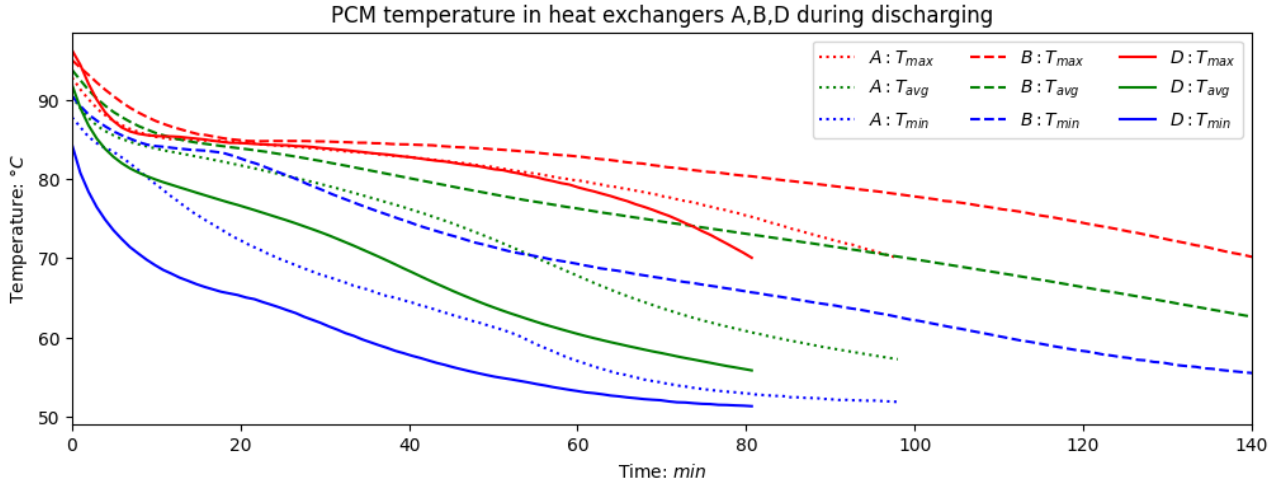

Figure 13. *The maximum (T_{max}), average (T_{avg}) and minimum (T_{min}) PCM temperature in heat exchangers A, B, and D during discharging.*

The heat flux presented in Figure 14, similarly to the charging process, reaches its highest value at the initial stage, amounting to approximately above 3.0 kW and 1.75 kW, respectively. It also exhibits a nonlinear character and asymptotically approaches values close to zero. At the same time, the shape of the curve is similar for heat exchangers A and B.

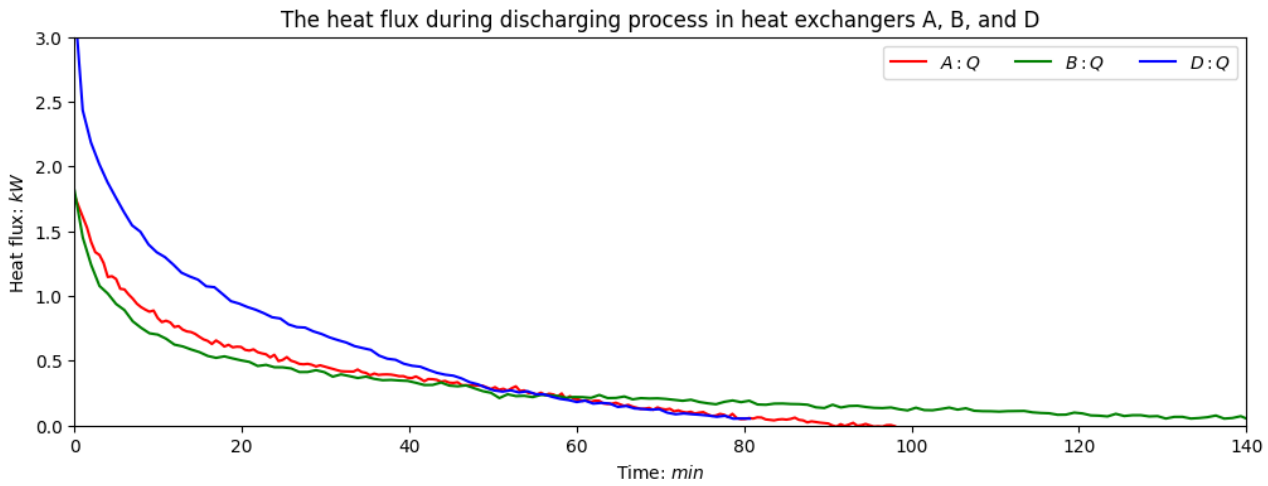

Figure 14. *The heat flux during discharging process in heat exchangers A, B, and D.*

3.3. Power and heat losses

Heat losses are very difficult to eliminate, despite the use of thermal insulation. Although they do not significantly affect the general shape of the performance characteristics, they substantially extend the charging process. Moreover, heat losses do not scale uniformly with increasing storage size. Therefore, for numerical analyses, it is necessary to separate heat losses from the model describing the behavior of the storage unit itself, so that they can be scaled independently in a separate model block. To determine the heat losses, the storage unit was brought to a steady state at a given temperature, and the power required to maintain this state was determined. Since the heat losses depend mainly on the ambient air temperature and the heat transfer surface area, the results were very similar for all tested heat exchangers. Subsequently, the relationship between heat losses and the average storage temperature was determined within the temperature range investigated in the previous experiments, and the heat exchanger power was corrected accordingly **Figure 15**.

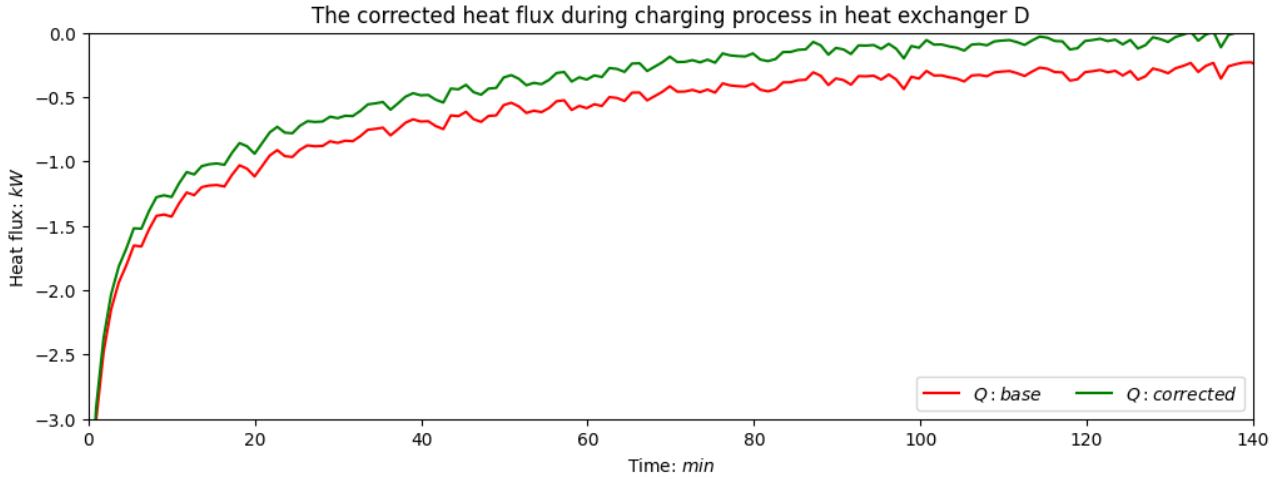

Figure 15. *The corrected heat flux during charging process in heat exchanger D.*

In dynamic analyses of the interaction between heat exchangers and external systems, one of the most important relationships is that between thermal power and the amount of stored energy. As stated earlier, this relationship differs for the charging and discharging processes. It is presented for both operating modes in **Figure 16**. After accounting for heat losses, the storage capacity obtained from the charging and discharging processes was consistent and could be described by the equations.

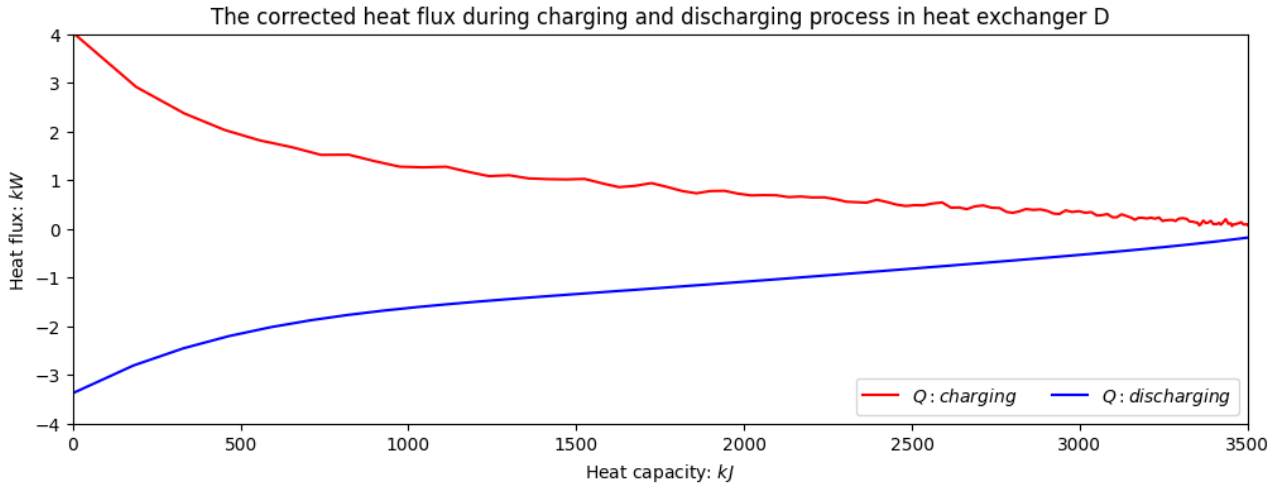

Figure 16. *The corrected heat flux during charging and discharging process in heat exchanger D.*

4. Conclusions

The conducted experiments made it possible to determine the behavior of the thermal energy storage unit during charging and discharging for different numbers of fins, which will enable the verification and improvement of numerical analyses aimed at modifying the storage unit design. As the number of fins increased, the thermal power also increased. At the same time, heat losses had a greater impact on the charging process when the power of the heat exchanger was lower. The power-versus-storage-capacity curves may be used in dynamic analyses of the interaction between thermal energy storage units and external systems. These power curves differ between the charging and discharging processes.

The study also showed that, for a larger amount of phase change material (10 kg), the melting and solidification processes are strongly influenced by volume change effects and convection. The former, combined with the tendency of the PCM to adhere to colder surfaces during solidification, leads to the formation of air voids, which negatively affect the subsequent charging process. Convection plays a particularly important role during charging. It causes thermal stratification inside the storage unit and leads to a condition in which the lower regions of the unit are difficult to heat sufficiently. This leads to the conclusion that the critical regions in the storage design are its extreme parts, namely the bottom during heating and the upper part during cooling, and particular attention should be paid to the heat exchanger design in these regions.

A second important conclusion from the study is that numerical simulations of such heat exchangers should not neglect shrinkage, viscosity, and convection effects, because omitting them at larger storage volumes may significantly distort the results.

Acknowledgments

This research was mainly supported by The National Centre for Research and Development, Poland - project “Opracowanie mobilnego magazynu ciepła pozwalaj ˛acego na wykorzystanie ciepła odpadowego dla spółki PTEP” Nowe Technologie w Zakresie Energii II (NTE-II/0004/2022), and partially supported by the Ministry of Science and Higher Education, Poland, grant AGH number 16.16.210.476.

Nomenclature

Symbols

c_p	specific heat capacity, kJ/(kg K)
$\dot{Q}$	heat flux, kW
$\dot{V}$	volumetric flow rate, m^3/s
T	temperature, °C

Greek symbols

ρ density, kg/m^3

Subscripts and superscripts

in inlet

out outlet

References

[1] Muzammal Islam M, Yu T, Giannoccaro G, Mi Y, la Scala M, Rajabi Nasab M, et al. Improving Reliability and Stability of the Power Systems: A Comprehensive Review on the Role of Energy Storage Systems to Enhance Flexibility. IEEE Access 2024;12:152738–65. https://doi.org/10.1109/ACCESS.2024.3476959.

[2] Chebli F, Mechighel F. Phase change materials: classification, use, phase transitions, and heat transfer enhancement techniques: a comprehensive review. J Therm Anal Calorim 2025;150:1353–411. https://doi.org/10.1007/s10973-024-13877-z.

[3] Mase Y, Sucipto ZF, Mobedi M. A numerical study on control mechanism of heat transfer in a double pipe PCM heat exchanger by changing eccentricity. Energy 2024;291:130266. https://doi.org/10.1016/j.energy.2024.130266.

[4] Choure BK, Alam T, Kumar R. Optimization of heat transfer in PCM based triple tube heat exchanger using multitudinous fins and eccentric tube. J Energy Storage 2024;102:113981. https://doi.org/10.1016/j.est.2024.113981.

[5] Pakalka S, Valančius K, Streckienė G. Experimental and Theoretical Investigation of the Natural Convection Heat Transfer Coefficient in Phase Change Material (PCM) Based Fin-and-Tube Heat Exchanger. Energies 2021;14:716. https://doi.org/10.3390/en14030716.

[6] Di Prima P, Santovito M, Papurello D. CFD Analysis of a Latent Thermal Storage System (PCM) for Integration with an Air-Water Heat Pump. Int J Energy Res 2024;2024. https://doi.org/10.1155/2024/6632582.

[7] Choure BK, Alam T, Kumar R. A review on heat transfer enhancement techniques for PCM based thermal energy storage system. J Energy Storage 2023;72:108161. https://doi.org/10.1016/j.est.2023.108161.

[8] He F, Hu C, Gao W, Li S, Meng X. Effect of inclination angles on heat transfer characteristics of solid and perforated spiral finned heat exchangers. Int Commun Heat Mass Transf 2025;164:108920. https://doi.org/10.1016/j.icheatmasstransfer.2025.108920.

[9] Marzouk SA, Aljabr A, Almehmadi FA, Sharaf MA, Alam T, Dobrotă D. Thermal performance enhancement of phase change material melting using innovative fins. Therm Sci Eng Prog 2025;61:103585. https://doi.org/10.1016/j.tsep.2025.103585.

[10] Rashid FL, Khalaf AF, Alizadeh A, Al-Obaidi MA, Salahshour S, Chan CK. Numerical investigation of the effect of the number of fins on the phase-change material melting inside a shell-and-tube cylindrical thermal energy storage. Case Stud Therm Eng 2024;60:104754. https://doi.org/10.1016/j.csite.2024.104754.

[11] Pássaro J, Rebola A, Coelho L, Conde J, Evangelakis GA, Prouskas C, et al. Effect of fins and nanoparticles in the discharge performance of PCM thermal storage system with a multi pass finned tube heat exchange. Appl Therm Eng 2022;212:118569. https://doi.org/10.1016/j.applthermaleng.2022.118569.

[12] PCM Products 2026. https://www.pcmproducts.net/ (accessed April 10, 2026).

[13] Kretzschmar H-J, Wagner W. International Steam Tables. Berlin, Heidelberg: Springer Berlin Heidelberg; 2019. https://doi.org/10.1007/978-3-662-53219-5.